Targeted deletion of the novel cytoplasmic dynein mD2LIC disrupts the embryonic organiser, formation of the body axes and specification of ventral cell fates

Amer Ahmed Rana[1,*,], Juan Pedro Martinez Barbera[1,†], Tristan A. Rodriguez[1,‡], Denise Lynch[1,§], Elizabeth Hirst[1], James C. Smith[2,*] and Rosa S. P. Beddington[1,¶]**

[1]Division of Mammalian Development, National Institute for Medical Research, The Ridgeway, Mill Hill, London NW7 1AA, UK
[2]Division of Developmental Biology, National Institute for Medical Research, The Ridgeway, Mill Hill, London NW7 1AA, UK
*Present address: Wellcome Trust/Cancer Research UK Gurdon Institute and Department of Zoology, University of Cambridge, Tennis Court Road, Cambridge, CB2 1QR, UK
†Present address: Neural Development Unit, Institute of Child Health, 30 Guilford Street, London, WC1N 1EH, UK
‡Present address: MRC Clinical Sciences Centre, Faculty of Medicine, Imperial College London, Hammersmith Hospital Campus, Du Cane Road, London, W12 0NN, UK
§Present address: Developmental Biology Program, Victor Chang Cardiac Research Institute, 384 Victoria Street, Darlinghurst, NSW 2010, Australia
¶Deceased 18 May 2001
**Author for correspondence (e-mail: a.rana@gurdon.cam.ac.uk)

Accepted 23 July 2004

Development 131, 4999-5007
Published by The Company of Biologists 2004
doi:10.1242/dev.01389

Summary

Dyneins have been implicated in left-right axis determination during embryonic development and in a variety of human genetic syndromes. In this paper, we study the recently discovered mouse dynein 2 light intermediate chain (*mD2LIC*), which is believed to be involved in retrograde intraflagella transport and which, like *left-right dynein*, is expressed in the node of the mouse embryo. Cells of the ventral node of mouse embryos lacking *mD2LIC* have an altered morphology and lack monocilia, and expression of *Foxa2* and *Shh* in this structure is reduced or completely absent. At later stages, consistent with the absence of nodal cilia, *mD2LIC* is required for the establishment of the left-right axis and for normal expression of *Nodal*, and the ventral neural tube fails to express *Shh*, *Foxa2* and *Ebaf*. *mD2LIC* also functions indirectly in the survival of anterior definitive endoderm and in the maintenance of the anterior neural ridge, probably through maintenance of *Foxa2*/*Hnf3β* expression. Together, our results indicate that *mD2LIC* is required to maintain or establish ventral cell fates and for correct signalling by the organiser and midline, and they identify the first embryonic function of a vertebrate cytoplasmic dynein.

Key words: D2LIC, Axis formation, Handedness, Mouse embryo, Intra-flagellar transport, Lefty2, Hnf3β

Introduction

Dynein is a large multi-subunit protein complex consisting of two heavy chains complexed to intermediate, light intermediate and/or light chains (Harrison and King, 2000). The dynein family has been divided into two subfamilies: the axonemal and cytoplasmic dyneins. Axonemal dyneins function as structural elements in cilia and flagella, and provide the force responsible for ciliary motion. By contrast, cytoplasmic dyneins are motor proteins involved in the intracellular transport of cargo along microtubules and in retrograde intra-flagellar transport during the assembly of cilia (Perrone et al., 2003).

The dyneins have been implicated in many cellular and developmental processes. For example, the gene responsible for the spontaneous classical mouse mutation *inversus viscerum* (*iv*) is an axonemal heavy chain dynein named left-right dynein (previously *lrd*; *Dnahc11* – Mouse Genome Informatics) (Supp et al., 1997). *Dnahc11* is expressed in the node of the mouse embryo and is necessary for the motility of cilia in the node. It is required for the establishment of the left-right body axis and has been implicated in Kartagener's and other immotile cilia syndromes (Supp et al., 1997). In addition, dyneins have been associated with severe clinical abnormalities, such as heterotaxia and isomerism (including polysplenia or asplenia), and with single organ inversions, such as dextrocardia (Casey and Hackett, 2000), as well as in human genetic disease syndromes including spinal bulbar muscular atrophy and spinal muscular atrophy (Hafezparast et al., 2003).

The importance of intra-flagellar transport in embryonic development has been emphasised by analysis of wimple (previously Wim; Ift172 – Mouse Genome Informatics) and flexo (previously Fxo; Tg737Rpw – Mouse Genome Informatics) (Huangfu et al., 2003), which, together with the kinesin Kif3a (Marszalek et al., 1999; Takeda et al., 1999), are involved in anterograde intra-flagellar transport. Mouse mutants lacking *Wim* or *Fxo* fail to specify ventral cell fates, probably because Shh signalling is disrupted downstream of the patched receptor (Huangfu et al., 2003).

Together, these observations emphasise that the study of dyneins is of great cellular, developmental and medical interest. Recently, on the basis of its amino acid sequence and

its ability to interact with cytoplasmic dynein 2 heavy chain (DHC2), Grissom and colleagues (Grissom et al., 2002) have classified dynein 2 light intermediate chain (D2LIC) as a novel member of the dynein family of proteins. Consistent with this proposal, XBX-1, the *Caenorhabditis elegans* homologue of D2LIC, proves to be required for retrograde intraflagellar transport (Schafer et al., 2003). We previously identified mouse *D2LIC* (*mD2LIC*; 4933404O11Rik – Mouse Genome Informatics) as a gene that is expressed in the node of the developing embryo (Sousa-Nunes et al., 2003), and in this paper we investigate its function during development. Our work shows that *mD2LIC* is needed to maintain or establish ventral cell fates, for monocilium formation in the ventral node, and for correct signalling by the organiser and midline. Our experiments define the first embryonic function for a vertebrate cytoplasmic dynein.

Materials and methods

In situ hybridisation

In situ hybridisation of *mD2LIC* was performed as described (Wilkinson and Nieto, 1993) using probes derived from EST clone AL024282. Probes specific for other genes are described in the text. The *lefty* probe (Meno et al., 1997) detects both *Leftb* (previously *lefty1*) and *Ebaf* (previously *lefty2*) transcripts.

Northern blot analysis

Total RNA was isolated from adult tissues and from 11.5 dpc whole embryos and placenta as described (Chomczynski and Sacchi, 1987). A probe was prepared from a full-length *mD2LIC* cDNA. Hybridisation was performed as described (Martinez-Barbera et al., 1997).

Scanning electron microscopy

Scanning electron microscopy was performed as described (Sulik et al., 1994), with 15 minutes uranyl acetate treatment.

TUNEL staining

TUNEL staining was performed as described (Barbera et al., 2002).

Gene targeting

Genomic clones were isolated from a 129/Olac genomic library (Stratagene) using an *mD2LIC* full-length cDNA to generate a probe. A 2.75 kb region of the endogenous genomic locus was replaced by homologous recombination in E14TG2A ES cells with a 2 kb *loxP* flanked PGK neomycin (*PGKneo*) cassette using a *diphtheria toxin A* (*DTA*) cassette for negative selection (Fig. 3). Correctly targeted cells from five independent cell lines were used to generate chimeric animals that were subsequently mated to produce heterozygous individuals. Only heterozygotes derived from the same cell line were intercrossed. The phenotypes of homozygous individuals derived from each of the five cell lines were similar, indicating that the embryonic defects observed in this paper are consequences of the targeting event.

Genotyping of wild-type and mutant m*D2LIC* alleles

Individuals were genotyped using the polymerase chain reaction (PCR) or by Southern blot analysis. In the PCR strategy, a 450 bp product specific to the wild-type locus was amplified using the primers P1 (5′-GCCCAACATTGTTTCAGCTTCC-3′) and P2 (5′-TGACA-GCGAGGTACTACTGCT-3′), and a 350 bp neomycin-specific PCR product was amplified using the primers 5′-CAAG-ATGGATTGCACGCAGG-3′ and 5′-CGGCAGGAGCAAGGTGA-GAT-3′. Southern blotting was performed as described using a 700 bp probe that lies externally to the targeted region and recognises 13 kb (wild-type locus) and 6 kb (targeted locus) genomic fragments following digestion with *Hin*dIII (see Fig. 3).

Results

Sequence and expression pattern of *mD2LIC*

In contrast to Grissom and colleagues (Grissom et al., 2002), we find that mD2LIC protein is predicted to contain 351 amino acids, with a putative P-loop (nucleotide binding domain) near its N terminus (Fig. 1). We believe that this discrepancy has arisen because Grissom and colleagues (Grissom et al., 2002) made use of an EST sequence (mouse locus AK008822, BAB25915; *M. musculus* Genome Sequencing Consortium) that contains a frame shift relative to the sequence presented in our study; when translated, this results in a 209 amino acid protein that lacks the P-loop domain. Our translation of the *mD2LIC* cDNA (Sousa-Nunes et al., 2003) yields a protein that closely resembles the 350 amino acid human D2LIC, such that there is 87% identity and 92% amino acid charge matches between the two proteins.

Expression of *mD2LIC* in the late streak to early somite stage mouse embryo is restricted to the monociliated cells of the ventral node (Sousa-Nunes et al., 2003) (Fig. 2A-E). Northern blot analysis reveals a single transcript of 1.4 kb, and in the adult strongest expression of *mD2LIC* occurs in kidney and brain (Fig. 2F). The initial expression pattern of *mD2LIC* resembles that of the axonemal *left-right dynein* (*lrd*), suggesting that *mD2LIC*, like *lrd*, is involved in establishment of the embryonic axis (Supp et al., 1999).

Targeted mutation of *mD2LIC*

To analyse the function of *mD2LIC*, we generated a targeted mutation in embryonic stem cells. The mutation results in loss of both transcriptional and translational start sites and is likely to represent a null allele (Fig. 3A-D). *mD2LIC*$^{-/-}$ mutants die before 11.5 days post coitum (dpc) (Table 1) and gross phenotypic effects are detectable from 8.5 dpc, with defects in notochord and floorplate formation and a reduction in definitive endoderm. These are followed by anterior truncations of the forebrain, defects in the ventral body wall and in closure of the neural tube, and either an arrest of embryonic turning and heart looping or a randomisation in their direction (Fig. 3E; Table 2). The severity of this phenotype varies from embryo to embryo, and we have defined three phenotypic classes (Fig. 3E; Table 2). Class I, the most severe, was observed most frequently, and our analysis therefore concentrates on such embryos unless stated otherwise.

The gross phenotype at 8.5 dpc and later is presaged at 7.5 dpc by a disruption of cilium formation in the ventral node, where expression of *mD2LIC* is highest. Although scanning electron microscopy revealed that the gross morphology of the node is normal in null mutants (Fig. 4A,C,E), the single cilium that is normally carried by ventral node cells was absent in four out of 12 null mutant embryos. A further eight embryos formed only stunted cilium-like structures that were restricted to the posterior region of the node (Fig. 4B,D,F-I). Cells of the notochordal plate lacked cilia completely, suggesting that the stunted cilium-like structures visible in the node of some embryos are later lost, perhaps through reabsorption. We note that cells in the node and notochordal

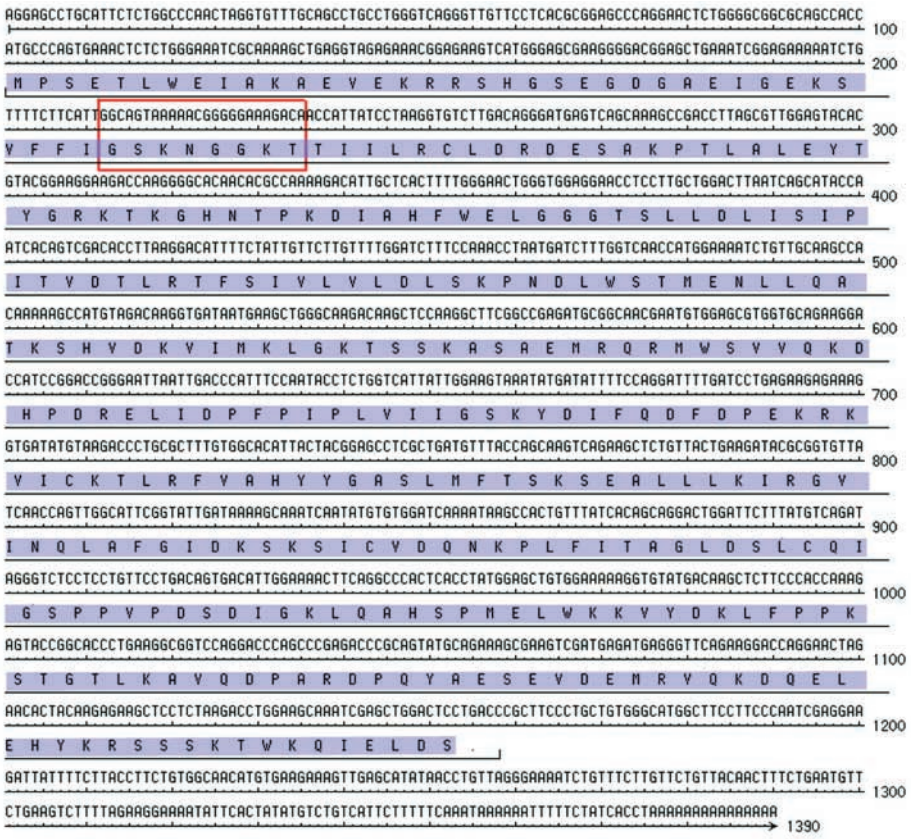

Fig. 1. cDNA sequence and translation of *mD2LIC*. The cDNA comprises 1390 bp and codes for a 351 amino acid protein predicted to contain a P-loop (nucleotide binding domain) near its N terminus (red box). This sequence differs from the previously published mD2LIC (Grissom et al., 2002), but the predicted protein resembles closely the rat and human gene products. We suspect that the previously published sequence contains a frame-shift near the 5′ end of the cDNA, resulting in a predicted protein of only 209 amino acids that lacks the P loop.

plate also appear flatter than their wild-type counterparts (Fig. 4B,D,F-I).

Gene expression patterns in *mD2LIC*$^{-/-}$ mutant embryos

The abnormal appearance of the node suggests that these cells might be incorrectly specified. To address this point, we examined the expression patterns of *Fgf8*, *Shh*, *T* and *Foxa2* (previously Hnf3β) (Ang and Rossant, 1994; Crossley and Martin, 1995; Echelard et al., 1993; Wilkinson et al., 1990). At the late streak stage, expression of *Fgf8* is normal in null mutant embryos (Fig. 5A,B), while expression of both *Shh* (*n*=5/5; Fig. 5C-E) and *T* (*n*=5/5; data not shown) is slightly reduced. Most significantly, expression of *Foxa2* in the region of the node was severely reduced in *mD2LIC*$^{-/-}$ embryos (*n*=7/9), and in some was almost undetectable (*n*=2/9) (Fig. 5F-J).

Gene expression patterns in derivatives of the node are also disrupted. *T* (Fig. 6A,B) and *Shh* (data not shown) are both expressed in a discontinuous manner in the region of the notochord, while *Foxa2* is completely absent here and in the floor plate of null mutant embryos, and its expression in foregut endoderm is markedly reduced (Fig. 6E,F). *Shh* transcripts are also absent from the floor plate and endoderm of *mD2LIC*$^{-/-}$ embryos (Fig. 6C,D). The downregulation of these genes is unlikely to be due to cell death; TUNEL staining revealed no abnormal levels of apoptosis in the node or its derivatives at any of the stages examined (Fig. 5K-M). Consistent with the downregulation of *T*, *Shh* and *Foxa2* in the midline of *mD2LIC*$^{-/-}$ embryos, histological analysis revealed that loss of mD2LIC impairs differentiation of the notochord (see Table 3).

Disruption of signalling by the node and axial mesoderm in *mD2LIC*$^{-/-}$ mutant embryos

The signalling properties of the node and axial mesendoderm

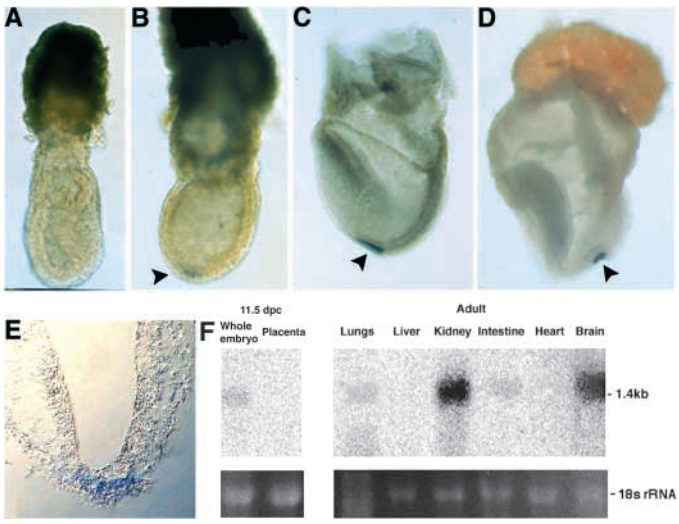

Fig. 2. Expression pattern of *mD2LIC*. Transcription of *mD2LIC* is not detected by in situ hybridisation before the onset of gastrulation (A), but from late streak (B) to headfold stages (C,D) transcription is observed in the node (black arrowheads). Sections reveal that this expression is restricted to cells of the ventral node (E). Northern blot analysis reveals a single transcript of 1.4 kb, and in the adult expression is highest in brain and kidney (E).

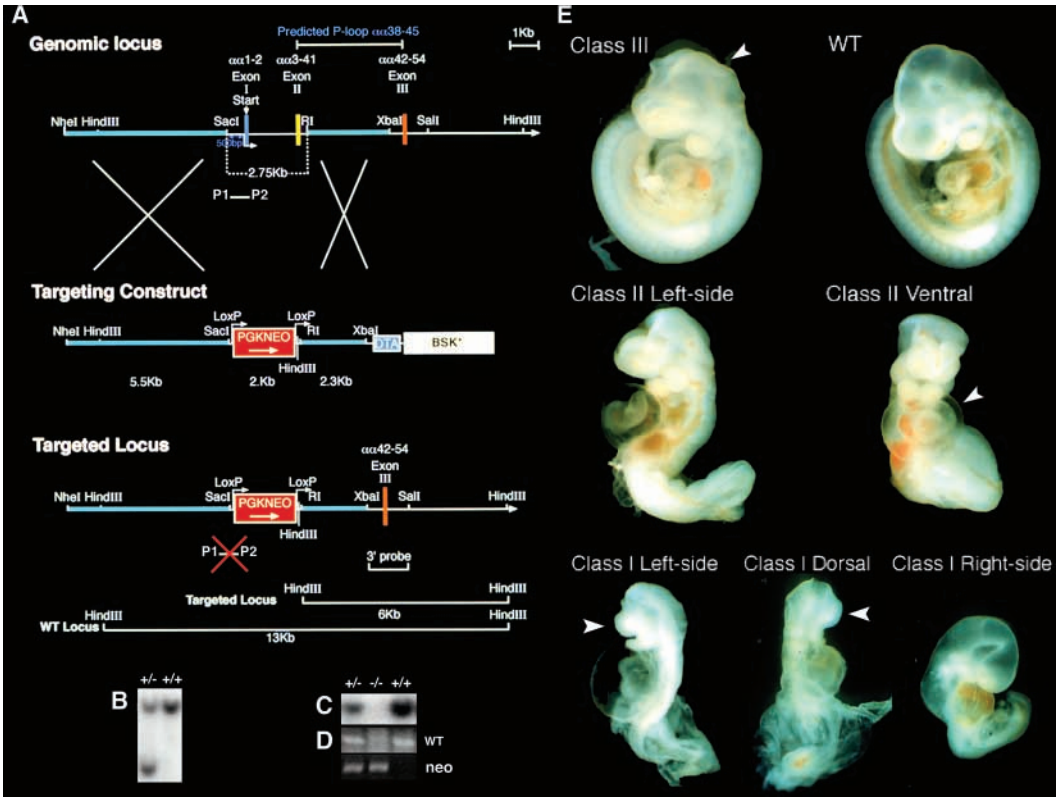

Fig. 3. Targeted deletion of *mD2LIC*. (A) The targeting strategy involved removing 2.75 kb of the endogenous *mD2LIC* locus. This contains 500 bp upstream of the predicted transcriptional start site together with the first two exons, which include the translation start site and half the P-loop domain. The targeting vector incorporates both positive (neomycin resistance) and negative (diphtheria toxin A) selection, and comprises a 5.5 kb 5′ homology arm, a 2 kb *loxP* flanked *PGKneo* cassette (which replaces the targeted region) and a 2.3 kb 3′ homology arm. During the targeting event, an exogenous *Hin*dIII restriction site is introduced into the locus just downstream of the *PGKneo* cassette. (B) Use of a 3′ probe in Southern blot analyses of transfected ES cell genomic DNA digested with *Hin*dIII reveals a 13 kb band corresponding to the wild-type locus and a 6 kb band representing a correctly targeted locus. (C) Northern blot analysis of littermates from heterozygous crosses demonstrates loss of the *mD2LIC* transcript in homozygous mutant individuals and a decrease in heterozygous animals. (D) Primers P1 and P2 (indicated in A), together with a pair of primers designed to detect *neo*, distinguish between targeted and non-targeted alleles when genotyping. (E) Classification of *mD2LIC*$^{-/-}$ mutants into three groups according to the extent of embryonic turning at 9.5 dpc (Table 1). Class I mutants (bottom, 61%; *n*=39), which exhibit the most severe phenotype, fail to initiate embryonic turning. Three examples are shown here. Class II (middle, 21%) mutants start but do not complete embryonic turning, and Class III (top, 18%) mutants complete turning but always display an open neural tube in the region of the head (arrowhead). Other defects include reversal of heart looping (Class II, white arrowhead), ballooning of the pericardial sac, anterior truncations (Class III, white arrowhead) and defects in truck and tail development.

in *mD2LIC*$^{-/-}$ mutant embryos, and the establishment of the left-right axis, were further investigated by examining the expression of *Nodal*, *Leftb*, *Ebaf* and *Pitx2* (Collignon et al., 1996; Kitamura et al., 1999; Meno et al., 1997). *Nodal* is the earliest known asymmetric marker of the left-right axis. In wild-type embryos expression first occurs symmetrically around the periphery of the node, but it then becomes asymmetrical, with higher levels and a broader domain of expression on the left-hand side. *nodal* is then also expressed in the left-hand lateral plate. At late streak stages *nodal* expression was reduced in three *mD2LIC*$^{-/-}$ embryos, was absent in one, and, in contrast to its normal expression pattern, was expressed symmetrically around the node in eight (Fig. 6G,H and data not shown). At later stages (2-5 somite stages), left-sided (*n*=2/9), right-sided (*n*=1/9) and bilateral (*n*=5/9) expression patterns were observed in the lateral plate, and in one embryo (*n*=1/9) no expression was detectable. We note that the frequency of bilateral expression is similar to the frequency of the more severe Class I and II mutants (Table 2). Expression of *Leftb* was undetectable in all null embryos (*n*=5/5), while *Ebaf* expression occurred bilaterally in three out of five embryos, was expressed on the right-hand side in another, and was absent in a fifth (Fig. 6L,M). Similar results were observed with *Pitx2* (Fig. 6N-Q). Together, these results indicate that

Table 1. Frequency of individuals recovered from heterozygous intercrosses

Stage (dpc)	Number of embryos	+/+ (%)	+/– (%)	–/– (%)
7.5	317	29	48	23
8.5	198	23	50	27
9.5	169	33	44	23
10.5	32	28	53	19
11.5	12	34	58	8
12.5	4	50	50	0
13.5	8	25	75	0

Table 2. Classification of homozygous mutant embryos at 9.5 dpc

Class	Frequency (*n*)	Anterior truncations (%)	Trunk/posterior reduction (%)	Neural tube closure defect (%)	Ventral closure defect (%)	Axial rotation defect (%)	Reversal of heart looping (%)	Ballooning of pericardial sac; oedema (%)
I	62% (24)	100	100	88	100	100	54	100
II	21% (8)	Variable	75	88	63	100	50	100
III	18% (7)	Variable	0	100	0	28	39	50

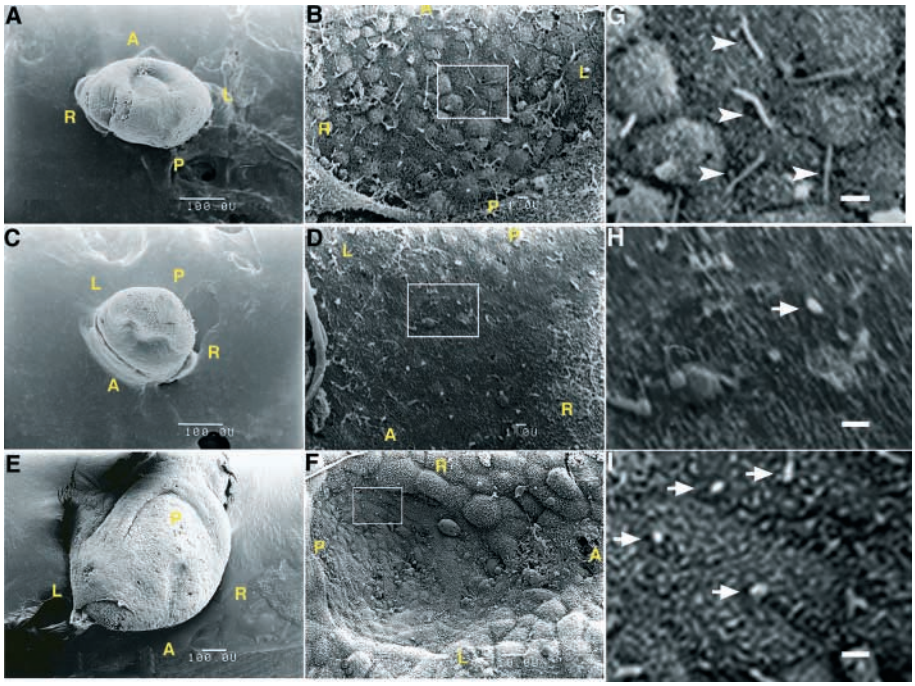

Fig. 4. Scanning electron microscopy reveals defects in monocilium formation in *mD2LIC*$^{-/-}$ mouse embryos. (A) The distal tip of a wild-type embryo at 7.5-8.0 dpc (1-2 somite stage) viewed at low power. (C,E) The gross morphology of the node of homozygous mutant embryos is normal. Conditions and magnification are identical in A and C, and E is at twice the magnification. (B,G) Higher-power view of a wild-type embryo reveals rounded cells bearing monocilia (arrowheads). (D,H,F,I) Ventral node cells in *mD2LIC*$^{-/-}$ embryos are flatter than their wild-type counterparts and they lack normal monocilia. In some cases stunted structures are formed in the place of monocilia (arrows). G-I are at the same magnification. White boxes in B,D,F indicate regions of the node shown at higher magnification in G-I respectively. (F) Cells in the anterior region of the node and notochordal plate have the most extreme phenotype.

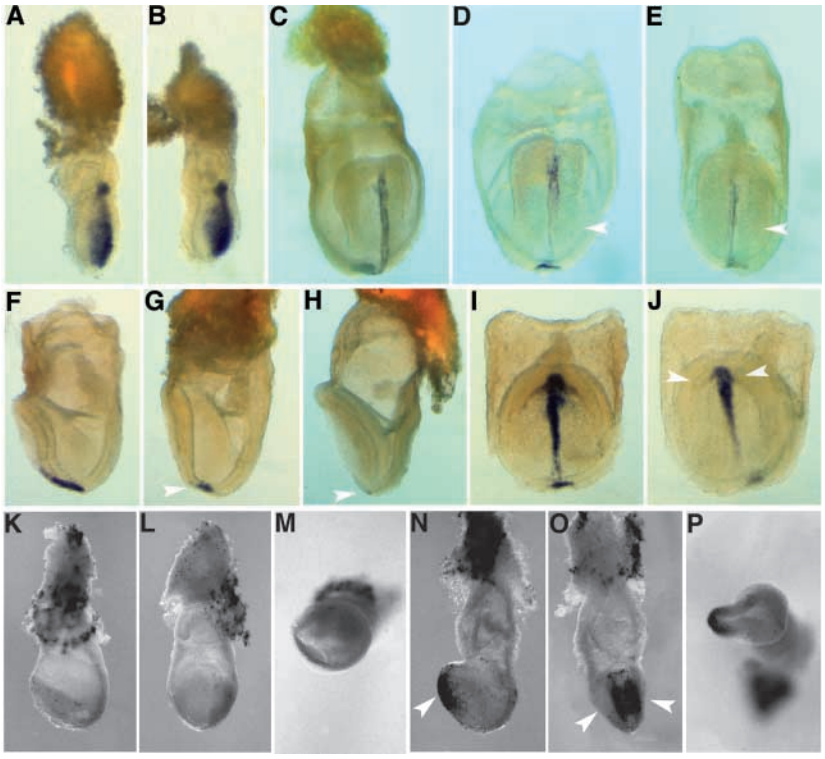

Fig. 5. Analysis of the *mD2LIC* phenotype at gastrula stages. (A,B) Expression of *Fgf8* is unaffected by loss of *mD2LIC* function. (A) Lateral view of wild-type embryo; (B) Lateral view of *mD2LIC*$^{-/-}$ embryo. (C-E) *Shh* expression is reduced in the node and axial mesoderm of *mD2LIC*-null mutants. (C) Wild-type embryo showing expression of *Shh* in the node and in axial structures. (D,E) Reduction of *Shh* expression (arrowheads) in *mD2LIC*$^{-/-}$ embryos. (F-J) Reduction in *Foxa2* expression in mD2LIC null mutant embryos. (F) Wild-type embryo showing expression of *Foxa2* in the node and axial mesendoderm. (G,H) Expression of *Foxa2* is severely reduced (G) or absent (H) in *mD2LIC*-null mutant embryos. (I,J) *Foxa2* expression is later reduced in anterior definitive endoderm in *mD2LIC*$^{-/-}$ embryos. (I) Wild-type embryo. (J) *mD2LIC*$^{-/-}$ embryo. Arrowheads mark anterior definitive endoderm. (K-P) TUNEL analysis of *mD2LIC*$^{-/-}$ embryos reveals no elevation of cell death in the node or its derivatives but apoptosis does occur in anterior definitive endoderm. (K-M) Little apoptosis is observed in the embryonic region of wild-type embryos at 7.5 dpc (K, lateral view; L, anterior view; M, distal view). In *mD2LIC*$^{-/-}$ embryos, no apoptosis is observed in the node or its derivatives (P) but substantial cell death occurs in the anterior definitive endoderm (arrowheads, N, lateral; O, anterior).

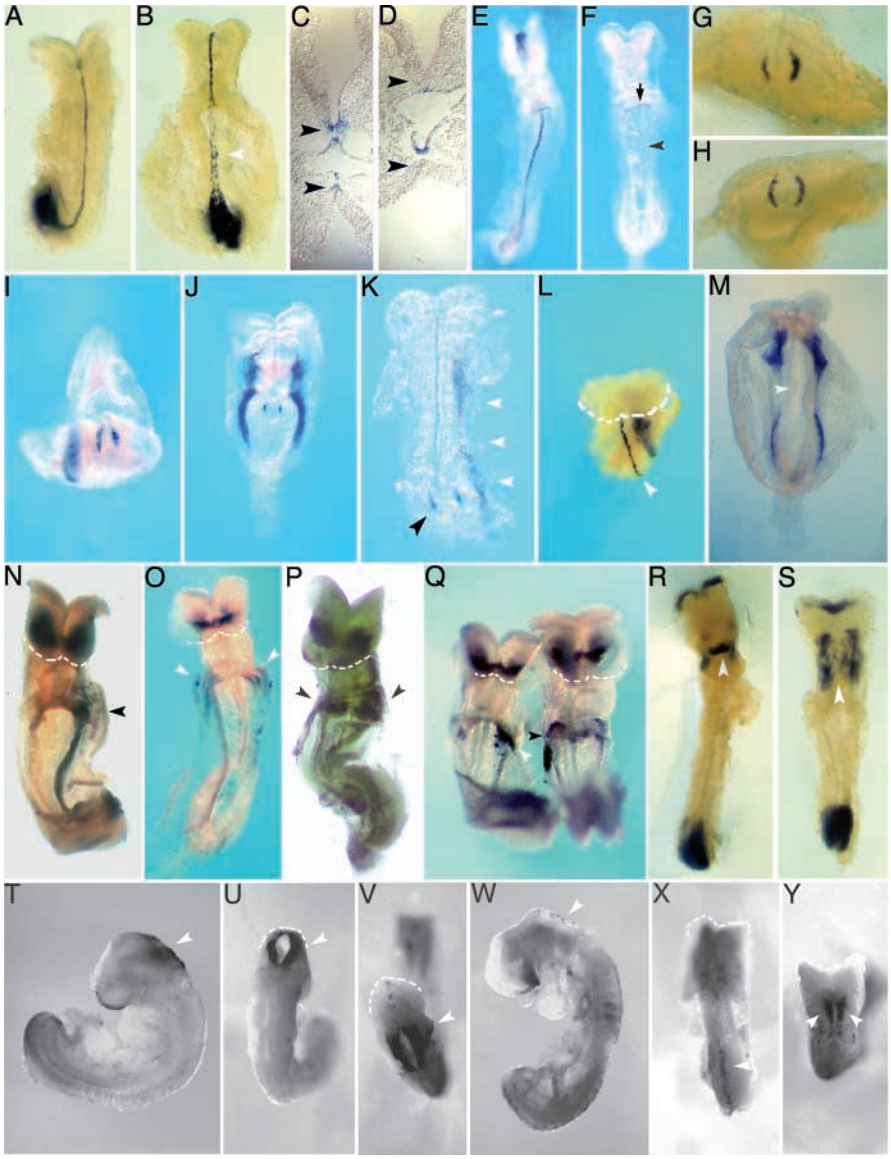

Fig. 6. Analysis of *mD2LIC*$^{-/-}$ mutants at 8.5-9.0 dpc. (A,B) Expression of T is discontinuous and distorted in the notochord of embryos lacking *mD2LIC*. (A) Wild-type embryo; (B) *mD2LIC*$^{-/-}$ embryo. (C,D) Expression of *Shh* is also discontinuous in null mutant embryos (data not shown) and is absent in the ventral neural tube as seen in histological sections (black arrowheads; sections shown here are from the head region). (C) Wild-type embryo; (D) *mD2LIC*$^{-/-}$ embryo. (E,F) mD2LIC-null embryos lack expression of *Foxa2* in notochord and ventral neural tube and expression is greatly reduced in definitive embryonic endoderm. (E) Wild-type embryo (ventral view); (F) mutant embryo (ventral view); *Foxa2* expression is lacking in notochord and ventral neural tube (arrowhead), and there is a reduction of expression in definitive endoderm (arrow). (G-Q) Defective establishment and maintenance of the left-right axis in *mD2LIC*$^{-/-}$ mutants. Wild-type (G, distal view) asymmetric expression of nodal around the node is not observed in null mutants (H, distal view). At the early somite stage, left-lateral plate specific expression of nodal (I, posterior view) is either expressed bilaterally (J, ventral view), on the right (K, dorsal view, white arrowheads; black arrowhead indicates expression in the node), on the left or absent (data not shown). Expression of *Leftb* in the left side of the ventral neural tube (L, anterior view, arrowhead; broken white line indicates the anterior edge of the head folds) is absent in null mutants (M, dorsal view, arrowhead) and *Ebaf* expression is randomised (in this case showing bilateral expression). Left lateral plate *Pitx2* specific expression (N, ventral view) is randomised in null mutants, appearing bilaterally in class I and II mutants (O,P, ventral view, arrowheads) or on the left (Q, left-hand embryo, ventral view, arrowhead) or on the right (Q, right-hand embryo, ventral view, arrow) in class III mutants. White lines indicate the boundary of the headfolds. (R,S) Lack of *Fgf8* expression in the anterior neural ridge (ANR) of *mD2LIC*$^{-/-}$ embryos. (R) Wild-type embryo (ventral view). Arrowhead shows expression of *Fgf8* in the ANR. (S) *mD2LIC*$^{-/-}$ mutant embryo (ventral view). *Fgf8* expression does not occur the in ANR (arrowhead). (T-Y) TUNEL staining reveals altered apoptotic profiles during neural tube closure. Normal apoptosis in the region of the hindbrain (arrowheads; T, lateral view; U, dorsal view of trunk; V, dorsal view of head) is absent in mutant (arrowhead in W, lateral view; X,Y, dorsal view). In addition, ectopic cell death is observed along the dorsal midline in mutants (X, dorsal view of trunk, arrowhead), but does not occur in wild-type littermates (U). Cell death is also observed in the cephalic mesoderm surrounding the notochord in the region of the head (arrowheads, Y).

left-right asymmetry is not generated correctly in *mD2LIC*$^{-/-}$ embryos, perhaps owing to the impairment of ciliogenesis and subsequent disruption of Nodal signalling, together with impaired development of the midline (see Discussion).

Anterior truncations and neural tube closure defects in *mD2LIC*$^{-/-}$ mutants

The later phenotypes observed in *mD2LIC* null embryos, such as anterior truncations and defects in neural tube closure, are likely to be consequences of the earlier defects. For example, expression of *Foxa2* in the anterior definitive endoderm of *mD2LIC*$^{-/-}$ mutants is greatly reduced (Fig. 5I,J), and this is accompanied by extensive cell death in this tissue (Fig. 5K-P). *mD2LIC* is not normally expressed in the anterior definitive endoderm, suggesting that these cells are deprived of a survival signal that is normally produced by the node or its derivatives. During normal development, the anterior definitive endoderm maintains an *Fgf8* signalling centre in the anterior neural ridge, which in turn is required for correct anterior development (Martinez Barbera et al., 2000; Shimamura and Rubenstein, 1997). *Fgf8* expression in the anterior neural ridge is significantly reduced in *mD2LIC*$^{-/-}$ mutants (Fig. 6R,S), presumably because of defects in the anterior definitive endoderm, and the decrease in *Fgf8* will lead to defects in anterior development (Fig. 7).

Defects in neural tube closure are also likely to be an indirect

Table 3. Analysis of notochord development in *mD2LIC*$^{-/-}$ mutant embryos

Stage	Wild type	Class I (notochord not always distinguishable)	Class II (notochord not always distinguishable)	Class III
1	5.8%	30.8%	19.3%	10.2%
2	35.3%	51.4%	43.5%	42.4%
3	59.9%	17.8%	41.2%	47.4%

Early notochord development can be subdivided into three stages: (1) formation of the notochordal plate; (2) condensation of the notochordal plate to form the notochord; and (3) separation of the notochord basement membrane from that of the endoderm. To characterise the notochord defect in detail, sections from between the level of the heart to the tail bud of 9.5 dpc *mD2LIC*$^{-/-}$ embryos were examined. These sections were obtained from representative embryos of all three classes, in order to determine how notochord development differs between the different classes of null mutants. Sections were stained by in situ hybridisation for expression of *T* (*n*=2) or with Haematoxylin and Eosin (*n*=2). The appearance of the notochord in each section was classified with respect to its membership one of the three stages outlined above.

consequence of loss of *mD2LIC*. Neural tube closure involves specification of the floor plate in response to signals derived from the notochord (Chen and Behringer, 1995; Huangfu et al., 2003; Wallingford and Harland, 2002) and modelling of the dorsal neural tube through apoptosis (Martinez Barbera et al., 2000); the process also requires mechanical support from adjacent cephalic mesenchyme (Weil et al., 1997). All these steps are likely to be affected in *mD2LIC*$^{-/-}$ embryos. Perhaps most significantly, reduced expression of *Shh* will prevent the notochord from acting as a normal signalling centre, thereby interfering with formation of the floorplate and with expression of *Foxa2*, *Shh* and *Ebaf*. In addition, however, TUNEL analysis at 9.0-9.5 dpc reveals that *mD2LIC*$^{-/-}$ embryos exhibit reduced levels of cell death in the hindbrain and also that there is ectopic cell death in the cephalic mesenchyme (Fig. 6T-Y). The elevated levels of apoptosis in the latter tissue may deprive the closing neural tube of its required mechanical support.

These and other aspects of the *mD2LIC*$^{-/-}$ phenotype are summarised in Fig. 7 and discussed below.

Discussion

The first detectable defect in mouse embryos lacking mD2LIC is a failure of cilium formation in the node (Fig. 4). The normal assembly of cilia involves two types of intraflagellar transport. During anterograde transport, protein particles are translocated to the tip of the growing cilium; this process requires the kinesins Kif3a and Kif3b in a heterotrimeric complex with kinesin-associated protein 3 (Cole et al., 1998; Morris and Scholey, 1997). The particles are conveyed back to the base of the cilium by retrograde transport, and as we discuss below, it is this process that requires cytoplasmic dyneins such as mD2LIC.

Evidence implicating cytoplasmic dyneins in retrograde transport comes from work in *Chlamydomonas* and *Caenorhabditis elegans*. *Chlamydomonas* lacking either dynein 2 heavy chain (DHC2) or dynein light chain (LC8) fail

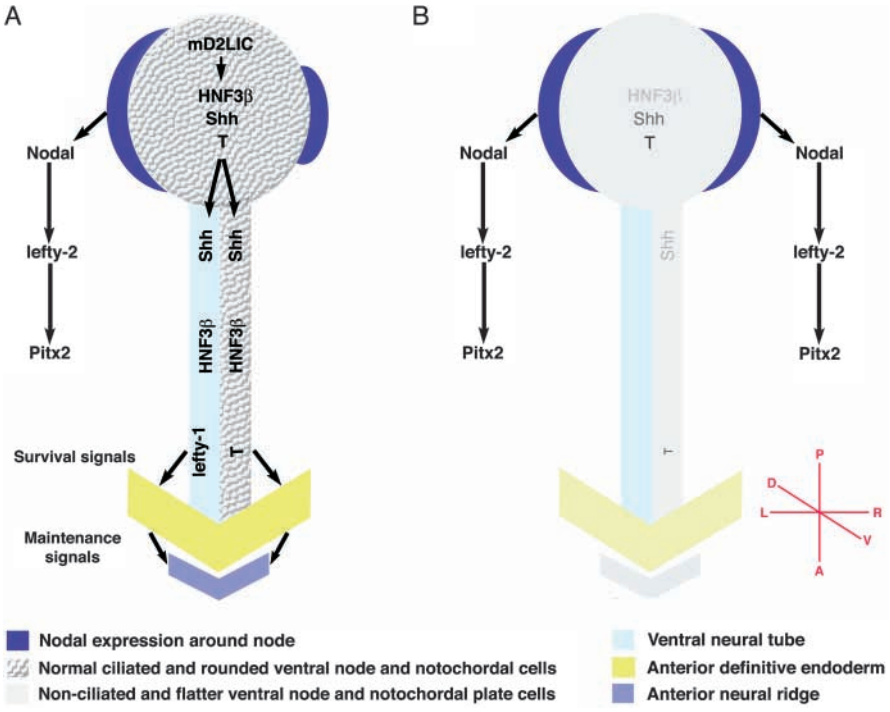

Fig. 7. A model for the function of *mD2LIC* in the establishment of the body axes. (A) In wild-type embryos, *mD2LIC* is required for the formation of cilia in the node and for the correct morphology of ventral node cells (mottled grey circle). It is also necessary for the normal expression of *Foxa2*, *Shh* and *T*, and for the asymmetric expression of *Nodal* (dark blue), which leads to the induction of *Nodal*, *Ebaf* and *Pitx2* in the left-hand-side of the embryo. The notochord (mottled rectangle below the node), also expresses *Foxa2*, *Shh* and *T*, while the adjacent ventral neural tube (light blue) expresses *Foxa2* and *Shh* and the nodal signalling antagonist *Leftb*. These structures constitute the midline, which is thought to act as a barrier to maintain left-right character in the developing embryo. The anterior definitive endoderm (ADE, yellow) receives survival signals from node derivatives, including the axial mesendoderm and ventral neural tube, and the ADE in turn is thought to maintain an *Fgf8*-expressing signalling centre in the anterior neural ridge (ANR, purple). This is required for maintenance of the forebrain and anterior identity. (B) In *mD2LIC*$^{-/-}$ mutants ventral node cells do not form cilia and are flatter than their wild-type counterparts (solid grey circle). Expression of *Foxa2*, *Shh* and *T* is severely reduced or absent (depicted as faded text) and expression of *Nodal* is usually symmetrical. The compromised signalling properties of the organiser result in reduced expression of *Shh*, *T* and *Foxa2* in the midline and consequently the absence of *Foxa2*, *Shh* and *Leftb* from the ventral neural tube. The bilaterally symmetrical expression of *Nodal* and the presumed loss of the midline barrier cause the nodal signalling pathway, normally active only in the left-hand side of the embryo, to be active on both sides. The defective axial mesendoderm does not emit survival signals to the ADE, and the *Fgf8* signalling centre in the ANR is lost.

to undergo normal ciliogenesis, and any cilium-like structures that do form are reabsorbed (Pazour et al., 1999; Pazour et al., 1998). mD2LIC can associate with DHC2 (Grissom et al., 2002; Perrone et al., 2003), suggesting that this cytoplasmic dynein is also involved in retrograde transport. Consistent with this idea, ciliogenesis is impaired in *C. elegans* lacking XBX-1, a homologue of D2LIC, and as in the *Chlamydomonas* mutants, those cilia that do form subsequently disappear, perhaps through reabsorption (Schafer et al., 2003). Together, these results suggest that loss of mD2LIC in the mouse node is directly responsible for the observed defects in cilium formation.

How does defective ciliogenesis lead to the mD2LIC$^{-/-}$ phenotype?

As discussed below, several aspects of the *mD2LIC* mutant phenotype may be due directly to the loss of cilia and a disruption of nodal flow. Other defects, however, such as the early downregulation of genes such as *Foxa2* and *Shh*, may have a more indirect aetiology. There may, for example, be a general impairment of cellular function: D2LIC is present in the Golgi apparatus and centrosomes (Grissom et al., 2002), and its loss may cause defects in protein maturation, in the cytoskeleton or in cell polarity.

Other elements of the *mD2LIC*$^{-/-}$ phenotype may result from a reduction in Hedgehog activity. The more severely affected *mD2LIC*$^{-/-}$ embryos resemble those deficient in Hedgehog signalling, such as the *Smo*$^{-/-}$ single mutant and *Shh*$^{-/-}$/*Ihh*$^{-/-}$ double mutants (Zhang et al., 2001). *mD2LIC*$^{-/-}$ individuals also resemble embryos lacking *nt*, rotatin or *Sil*, as well as chimeric and conditional *Foxa2*$^{-/-}$ embryos (Dufort et al., 1998; Faisst et al., 2002; Hallonet et al., 2002; Izraeli et al., 1999; Melloy et al., 1998). Like *mD2LIC*$^{-/-}$ embryos, many of these mutants lack midline expression of *Foxa2*, one consequence of which would be a downregulation of *Shh* (Filosa et al., 1997).

It is possible that some of the later elements of the *mD2LIC*$^{-/-}$ phenotype are also consequences of defects in the Hedgehog signal transduction pathway. The phenotypes of our least severe 'Class III' embryos resemble those of embryos lacking the intra-flagellar transport proteins Kif3a, Wim, Polaris and Fxo, in all of which the neural tube fails to close in the region of the head (Huangfu et al., 2003; Takeda et al., 1999). This is a characteristic of embryos that lack *Shh* (Huangfu et al., 2003) and it is possible that *mD2LIC*$^{-/-}$ individuals, such as *Wim*$^{-/-}$, *Polaris*$^{-/-}$ and *Fxo*$^{-/-}$ embryos, are defective in Shh signal transduction as well as in *Shh* expression.

Finally, and as mentioned above, the lack of nodal cilia in *mD2LIC*$^{-/-}$ mice would be expected to interfere with nodal flow, and therefore with specification of the left-right axis. In the nodal flow hypothesis (Nonaka et al., 1998), cilia have been suggested to cause the unidirectional flow of a morphogen that thereby accumulates on just one side of the node and activates gene expression in an asymmetric fashion. More complicated models involve two populations of node monocilia, in which one population generates a fluid flow and the other senses and transduces it, thereby leading to an asymmetric calcium signal at the left-hand-side of the node (McGrath et al., 2003; Tabin and Vogan, 2003).

The absence of nodal cilia would disrupt asymmetric gene expression and thereby set in train the series of events that cause the defects we observe in *mD2LIC*$^{-/-}$ embryos. These events are described in Fig. 7, and include the decreased or symmetrical expression of genes such as *Nodal*, as well as the downregulation of *T*, *Foxa2* and *Shh*. They culminate in the requirement for *mD2LIC* in the survival of the anterior definitive endoderm and thereby for maintenance of the anterior neural ridge and for normal anterior development. Models involving maintenance of the anterior neural ridge by anterior definitive endoderm have been proposed previously (Camus et al., 2000; Hallonet et al., 2002), although this is the first time that defects in axial mesendoderm have been shown to lead to cell death in the anterior definitive endoderm.

Regulation of mD2LIC

Recent work has demonstrated that expression of *mD2LIC* is downregulated in Rfx3-deficient mouse embryos, and that these embryos too show defects in cilium development and left-right axis specification (Bonnafe et al., 2004). Expression of *mD2LIC* is not completely absent in *Rfx3*$^{-/-}$ individuals, however, and the phenotype of such mice is not as severe as that of our *mD2LIC* mutants, suggesting that other proteins also regulate *mD2LIC* expression.

This work was supported by the Medical Research Council and is dedicated to Rosa Beddington – much loved and missed. The authors thank members of the Divisions of Mammalian Development, Developmental Biology and Developmental Neurobiology, especially Simon Bullock, Jonathan Cooke, Sally Dunwoodie, Alex Gould, Shankar Srinivas and Derek Stemple, for helpful discussions. We are also grateful to Melanie Clements for technical assistance and to the staff of the Dunkin Green building for looking after the mice.

References

Ang, S. L. and Rossant, J. (1994). HNF-3 beta is essential for node and notochord formation in mouse development. *Cell* **78**, 561-574.

Barbera, J. P., Rodriguez, T. A., Greene, N. D., Weninger, W. J., Simeone, A., Copp, A. J., Beddington, R. S. and Dunwoodie, S. (2002). Folic acid prevents exencephaly in Cited2 deficient mice. *Hum. Mol. Genet.* **11**, 283-293.

Bonnafe, E., Touka, M., AitLounis, A., Baas, D., Barras, E., Ucla, C., Moreau, A., Flamant, F., Dubruille, R., Couble, P. et al. (2004). The transcription factor RFX3 directs nodal cilium development and left-right asymmetry specification. *Mol. Cell. Biol.* **24**, 4417-4427.

Camus, A., Davidson, B. P., Billiards, S., Khoo, P., Rivera-Perez, J. A., Wakamiya, M., Behringer, R. R. and Tam, P. P. (2000). The morphogenetic role of midline mesendoderm and ectoderm in the development of the forebrain and the midbrain of the mouse embryo. *Development* **127**, 1799-1813.

Casey, B. and Hackett, B. P. (2000). Left-right axis malformations in man and mouse. *Curr. Opin. Genet. Dev.* **10**, 257-261.

Chen, Z. F. and Behringer, R. R. (1995). twist is required in head mesenchyme for cranial neural tube morphogenesis. *Genes Dev.* **9**, 686-699.

Chomczynski, P. and Sacchi, N. (1987). Single-step method of RNA isolation by acid guanidinium thiocyanate-phenol-chloroform extraction. *Anal. Biochem.* **162**, 156-159.

Cole, D. G., Diener, D. R., Himelblau, A. L., Beech, P. L., Fuster, J. C. and Rosenbaum, J. L. (1998). Chlamydomonas kinesin-II-dependent intraflagellar transport (IFT): IFT particles contain proteins required for ciliary assembly in Caenorhabditis elegans sensory neurons. *J. Cell Biol.* **141**, 993-1008.

Collignon, J., Varlet, I. and Robertson, E. J. (1996). Relationship between asymmetric nodal expression and the direction of embryonic turning. *Nature* **381**, 155-158.

Crossley, P. H. and Martin, G. R. (1995). The mouse Fgf8 gene encodes a family of polypeptides and is expressed in regions that direct outgrowth and patterning in the developing embryo. *Development* **121**, 439-451.

Dufort, D., Schwartz, L., Harpal, K. and Rossant, J. (1998). The transcription factor HNF3beta is required in visceral endoderm for normal primitive streak morphogenesis. *Development* **125**, 3015-3025.

Echelard, Y., Epstein, D. J., St-Jacques, B., Shen, L., Mohler, J., McMahon, J. A. and McMahon, A. P. (1993). Sonic hedgehog, a member of a family of putative signaling molecules, is implicated in the regulation of CNS polarity. *Cell* **75**, 1417-1430.

Faisst, A. M., Alvarez-Bolado, G., Treichel, D. and Gruss, P. (2002). Rotatin is a novel gene required for axial rotation and left-right specification in mouse embryos. *Mech. Dev.* **113**, 15-28.

Filosa, S., Rivera-Perez, J. A., Gomez, A. P., Gansmuller, A., Sasaki, H., Behringer, R. R. and Ang, S. L. (1997). Goosecoid and HNF-3beta genetically interact to regulate neural tube patterning during mouse embryogenesis. *Development* **124**, 2843-2854.

Grissom, P. M., Vaisberg, E. A. and McIntosh, J. R. (2002). Identification of a novel light intermediate chain (D2LIC) for mammalian cytoplasmic dynein 2. *Mol. Biol. Cell* **13**, 817-829.

Hafezparast, M., Klocke, R., Ruhrberg, C., Marquardt, A., Ahmad-Annuar, A., Bowen, S., Lalli, G., Witherden, A. S., Hummerich, H., Nicholson, S. et al. (2003). Mutations in dynein link motor neuron degeneration to defects in retrograde transport. *Science* **300**, 808-812.

Hallonet, M., Kaestner, K. H., Martin-Parras, L., Sasaki, H., Betz, U. A. and Ang, S. L. (2002). Maintenance of the specification of the anterior definitive endoderm and forebrain depends on the axial mesendoderm: a study using HNF3beta/Foxa2 conditional mutants. *Dev. Biol.* **243**, 20-33.

Harrison, A. and King, S. M. (2000). The molecular anatomy of dynein. *Essays Biochem.* **35**, 75-87.

Huangfu, D., Liu, A., Rakeman, A. S., Murcia, N. S., Niswander, L. and Anderson, K. V. (2003). Hedgehog signalling in the mouse requires intraflagellar transport proteins. *Nature* **426**, 83-87.

Izraeli, S., Lowe, L. A., Bertness, V. L., Good, D. J., Dorward, D. W., Kirsch, I. R. and Kuehn, M. R. (1999). The SIL gene is required for mouse embryonic axial development and left-right specification. *Nature* **399**, 691-694.

Kitamura, K., Miura, H., Miyagawa-Tomita, S., Yanazawa, M., Katoh-Fukui, Y., Suzuki, R., Ohuchi, H., Suehiro, A., Motegi, Y., Nakahara, Y. et al. (1999). Mouse Pitx2 deficiency leads to anomalies of the ventral body wall, heart, extra- and periocular mesoderm and right pulmonary isomerism. *Development* **126**, 5749-5758.

Marszalek, J. R., Ruiz-Lozano, P., Roberts, E., Chien, K. R. and Goldstein, L. S. (1999). Situs inversus and embryonic ciliary morphogenesis defects in mouse mutants lacking the KIF3A subunit of kinesin-II. *Proc. Natl. Acad. Sci. USA* **96**, 5043-5048.

Martinez-Barbera, J. P., Vila, V., Valdivia, M. M. and Castrillo, J. L. (1997). Molecular cloning of gilthead seabream (Sparus aurata) pituitary transcription factor GHF-1/Pit-1. *Gene* **185**, 87-93.

Martinez Barbera, J. P., Clements, M., Thomas, P., Rodriguez, T., Meloy, D., Kioussis, D. and Beddington, R. S. (2000). The homeobox gene Hex is required in definitive endodermal tissues for normal forebrain, liver and thyroid formation. *Development* **127**, 2433-2445.

McGrath, J., Somlo, S., Makova, S., Tian, X. and Brueckner, M. (2003). Two populations of node monocilia initiate left-right asymmetry in the mouse. *Cell* **114**, 61-73.

Melloy, P. G., Ewart, J. L., Cohen, M. F., Desmond, M. E., Kuehn, M. R. and Lo, C. W. (1998). No turning, a mouse mutation causing left-right and axial patterning defects. *Dev. Biol.* **193**, 77-89.

Meno, C., Ito, Y., Saijoh, Y., Matsuda, Y., Tashiro, K., Kuhara, S. and Hamada, H. (1997). Two closely-related left-right asymmetrically expressed genes, lefty-1 and lefty-2: their distinct expression domains, chromosomal linkage and direct neuralizing activity in Xenopus embryos. *Genes Cells* **2**, 513-524.

Morris, R. L. and Scholey, J. M. (1997). Heterotrimeric kinesin-II is required for the assembly of motile 9+2 ciliary axonemes on sea urchin embryos. *J. Cell Biol.* **138**, 1009-1022.

Nonaka, S., Tanaka, Y., Okada, Y., Takeda, S., Harada, A., Kanai, Y., Kido, M. and Hirokawa, N. (1998). Randomization of left-right asymmetry due to loss of nodal cilia generating leftward flow of extraembryonic fluid in mice lacking KIF3B motor protein. *Cell* **95**, 829-837.

Pazour, G. J., Wilkerson, C. G. and Witman, G. B. (1998). A dynein light chain is essential for the retrograde particle movement of intraflagellar transport (IFT). *J. Cell Biol.* **141**, 979-992.

Pazour, G. J., Dickert, B. L. and Witman, G. B. (1999). The DHC1b (DHC2) isoform of cytoplasmic dynein is required for flagellar assembly. *J. Cell Biol.* **144**, 473-481.

Perrone, C. A., Tritschler, D., Taulman, P., Bower, R., Yoder, B. K. and Porter, M. E. (2003). A novel Dynein light intermediate chain colocalizes with the retrograde motor for intraflagellar transport at sites of axoneme assembly in chlamydomonas and Mammalian cells. *Mol. Biol. Cell* **14**, 2041-2056.

Schafer, J. C., Haycraft, C. J., Thomas, J. H., Yoder, B. K. and Swoboda, P. (2003). XBX-1 encodes a dynein light Intermediate chain required for retrograde intraflagellar transport and cilia assembly in *Caenorhabditis elegans*. *Mol. Biol. Cell* **14**, 2057-2070.

Shimamura, K. and Rubenstein, J. L. (1997). Inductive interactions direct early regionalization of the mouse forebrain. *Development* **124**, 2709-2718.

Sousa-Nunes, R., Rana, A., Kettleborough, R., Brickman, J. M., Clements, M., Forrest, A., Grimmond, S., Avner, P., Smith, J. C., Dunwoodie, S. L. et al. (2003). Characterising embryonic gene expression patterns in the mouse using non-redundant sequence-based selection. *Genome Res.* **13**, 2609-2620.

Sulik, K., Dehart, D. B., Iangaki, T., Carson, J. L., Vrablic, T., Gesteland, K. and Schoenwolf, G. C. (1994). Morphogenesis of the murine node and notochordal plate. *Dev. Dyn.* **201**, 260-278.

Supp, D. M., Witte, D. P., Potter, S. S. and Brueckner, M. (1997). Mutation of an axonemal dynein affects left-right asymmetry in inversus viscerum mice. *Nature* **389**, 963-966.

Supp, D. M., Brueckner, M., Kuehn, M. R., Witte, D. P., Lowe, L. A., McGrath, J., Corrales, J. and Potter, S. S. (1999). Targeted deletion of the ATP binding domain of left-right dynein confirms its role in specifying development of left-right asymmetries. *Development* **126**, 5495-5504.

Tabin, C. J. and Vogan, K. J. (2003). A two-cilia model for vertebrate left-right axis specification. *Genes Dev.* **17**, 1-6.

Takeda, S., Yonekawa, Y., Tanaka, Y., Okada, Y., Nonaka, S. and Hirokawa, N. (1999). Left-right asymmetry and kinesin superfamily protein KIF3A: new insights in determination of laterality and mesoderm induction by kif3A–/– mice analysis. *J. Cell Biol.* **145**, 825-836.

Wallingford, J. B. and Harland, R. M. (2002). Neural tube closure requires Dishevelled-dependent convergent extension of the midline. *Development* **129**, 5815-5825.

Weil, M., Jacobson, M. D. and Raff, M. C. (1997). Is programmed cell death required for neural tube closure? *Curr. Biol.* **7**, 281-284.

Wilkinson, D. G. and Nieto, M. A. (1993). Detection of messenger RNA by in situ hybridization to tissue sections and whole mounts. *Methods Enzymol.* **225**, 361-373.

Wilkinson, D. G., Bhatt, S. and Herrmann, B. G. (1990). Expression pattern of the mouse T gene and its role in mesoderm formation. *Nature* **343**, 657-659.

Zhang, X. M., Ramalho-Santos, M. and McMahon, A. P. (2001). Smoothened mutants reveal redundant roles for Shh and Ihh signaling including regulation of L/R symmetry by the mouse node. *Cell* **106**, 781-792.